

Linear bands, zero-momentum Weyl semimetal, and topological transition in skutterudite-structure pnictides

V. Pardo

Departamento de Física Aplicada, Universidade Santiago de Compostela, Spain, and Department of Physics, University of California Davis

J. C. Smith and W. E. Pickett

Department of Physics, University of California Davis

It was reported earlier [Phys. Rev. Lett. 106, 056401 (2011)] that the skutterudite structure compound CoSb_3 displays a unique band structure with a topological transition versus a symmetry-preserving sublattice (Sb) displacement very near the structural ground state. The transition is through a massless Dirac-Weyl semimetal, point Fermi surface phase which is unique in that (1) it appears in a three dimensional crystal, (2) the band critical point occurs at $k=0$, and (3) linear bands are degenerate with conventional (massive) bands at the critical point (before inclusion of spin-orbit coupling). Further interest arises because the critical point separates a conventional (trivial) phase from a topological phase. In the native cubic structure this is a zero-gap topological semimetal; we show how spin-orbit coupling and uniaxial strain converts the system to a topological insulator (TI). We also analyze the origin of the linear band in this class of materials, which is the characteristic that makes them potentially useful in thermoelectric applications or possibly as transparent conductors. We characterize the formal charge as $\text{Co}^+ d^8$, consistent with the gap, with its 3 site symmetry, and with its lack of moment. The Sb states are characterized as p_x (separately, p_y) σ -bonded Sb_4 ring states occupied and the corresponding antibonding states empty. The remaining (locally) p_z orbitals form molecular orbitals with definite parity centered on the empty $2a$ site in the skutterudite structure. Eight such orbitals must be occupied; the one giving the linear band is an odd orbital singlet A_{2u} at the zone center. We observe that the provocative linearity of the band within the gap is a consequence of the aforementioned near-degeneracy, which is also responsible for the small band gap.

PACS numbers:

I. MOTIVATION AND INTRODUCTION

Recent years have seen an explosion of interest in two areas that, while distinct in themselves, have also found some areas of overlap. One is the situation where Dirac-Weyl linear bands emanate from a point Fermi surface (FS), the so-called Dirac point. While linear bands around symmetry points are not uncommon in crystal structures, it is uncommon that such points can determine the Fermi energy (E_F), which is what happens in the celebrated case of graphene. It is necessary that there is a gap throughout the Brillouin zone except for the touching bands. Point FSs occur also in the case of conventional (massive) zero-gap semiconductors,¹ and give rise to properties that have been studied in some detail. The case of the Dirac-Weyl semimetal (point Fermi surface) systems is quite different,^{2,3} leading to a great deal of new phenomenology.

The other new and active area relevant to this paper is that of topological insulators (TIs), in which the Brillouin zone integral of a certain ‘gauge field’ derived from the k -dependence of the periodic part of the Bloch states of the crystal is non-vanishing.⁴⁻⁶ These integer-valued topological invariants delineate

TIs from conventional (‘trivial’) insulators, with distinctive properties that are manifested primarily in edge states.^{5,7-9} Identification of TIs, and study of their properties and the critical point that separates the phases, is highlighting new basic physics and several potential applications.

Recently we reported¹⁰ on the skutterudite structure compound CoSb_3 , which combines and interrelates several of these properties (Dirac-Weyl semimetal at $k=0$; critical point of degeneracy with massive bands; transition to topological insulator) in a unique way. The skutterudite structure, which is illustrated in Fig. 1 and is discussed in Sec. II, is critical to the electronic behavior in CoSb_3 though it may not be necessary for the unique type of critical point that arises. The relevant portion of the band structure, in a very small volume of the Brillouin zone (BZ) centered at Γ , is unusually simple compared to most of the TIs that have been discovered, *viz.* the Bi_2Se_3 class,¹¹ the HgTe class,¹² and the three dimensional system HgCr_2Se_4 .¹³

The electronic structure of skutterudites was studied early on by Singh and Pickett,¹⁴ who focused on the peculiar valence band which was linear (except exceedingly near Γ) and whose linearity extended surprisingly far out into the BZ. It became clear

that the linearity of the band was responsible for the large thermopower¹⁵ that is potentially useful in thermoelectric applications.^{16,17} The origin of the linearity was however not identified, but it leads to peculiar consequences:¹⁴ the density of states varies as ε^2 near the band edge rather than the usual three dimensional (3D) form $\sqrt{\varepsilon}$; as a consequence the carrier density scales differently with Fermi energy ε_F ; the inverse mass tensor $\nabla\nabla\varepsilon_k$ is entirely off-diagonal corresponding to an “infinite” transport mass; the cyclotron mass differs from conventional 3D behavior, etc. As the Sb sublattice is shifted in a symmetry-preserving way,¹⁰ the small semiconducting gap of CoSb_3 closes at a critical point, giving rise to an unusual occurrence: a Dirac-Weyl point in a 3D solid at the Γ point. This transition point sets the stage for a conventional insulator to topological insulator transition, although the specific behavior of the system at this point was not spelled out in our earlier work. The only other topological insulator phases in skutterudite materials that we are aware of are the examples by Jung *et al.*¹⁸ in $\text{CeOs}_4\text{Pn}_{12}$ filled skutterudites.

This paper is organized as follows. In Section II the skutterudite structure and its relation to the symmetric perovskite (ReO_3) structure is reviewed. The computational methods are outlined in Section III. Section IV discusses the evolution of the band structure during a perovskite-to-skutterudite transformation, including the development of the gap and the appearance of the linear band. Section V is devoted to constructing a microscopic but transparent understanding of the electronic structure, including the development of the energy gap and the character of the peculiar linear band and the lower conduction band triplet that it interacts with near, at, and beyond the critical point. In Section VI we provide details of the band inversion leading to the topological transition, and analyze the anisotropy at the critical point. A brief summary is provided in Sec. VII.

II. STRUCTURE AND RELATION TO PEROVSKITE

It is useful for the purposes of this paper to consider the skutterudite structure to be a strongly distorted perovskite (ATPn_3) structure in which the A atom is missing (*i.e.* the ReO_3 structure) and the interconnected TPn_6 octahedra are rotated substantially (T = transition metal; Pn = pnictogen). The skutterudite structure,^{20–22} pictured in Fig. 1, has space group $Im\bar{3}$ (#204) and a body-centered cubic (bcc) Bravais lattice, and is comprised of a bcc rep-

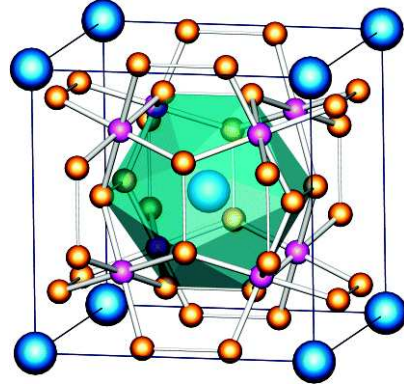


FIG. 1: (Color online) Crystal structure of skutterudite minerals (*viz.* CoSb_3) with space group $Im\bar{3}$ (#204), which includes inversion. The Co site (small pink [dark grey] sphere) is octahedrally coordinated to Sb atoms (small yellow [light gray] spheres). Each Sb atom connects two octahedra, as in the perovskite structure which has the same connectivity of octahedra. The large (blue) sphere denotes a large open site that is unoccupied in CoSb_3 but is occupied in filled skutterudites (see for example Ref. [19]). The geometrical solid (center of figure) provides an indication of the volume and shape of the empty region.

etition of four formula units (f.u.) when expressed as TPn_3 . The pnictide (Pn) atoms form bonded units (nearly square but commonly designated as “rings”) which are not required by local environment or overall symmetry to be truly square. The three Pn_4 squares in the primitive cell are oriented perpendicular to the coordinate axes. Transition metal (T) atoms (usually in the Co column) lie in six of the subcubes of the large cube of lattice constant a ; the other two subcubes (octants) are empty. The structure has inversion symmetry and is symmorphic, with 24 point group operations. The cubic operation that is missing is reflection in (110) planes. The related filled skutterudites $\text{XT}_4\text{Pn}_{12}$ have an atom X incorporated into the large $2a$ site of $3\bar{m}$ symmetry²³ that remains empty in the compounds that we discuss.

Figure 2 illustrates two aspects of the structure. The top panel reveals that, although the Sb_6 octahedra are rotated considerably (and strained) compared to the perovskite structure, a great deal of regularity is retained. The bottom panel gives a picture of the relationship between the Co atoms and the six Sb_4 rings that it is coordinated with (only three mutually orthogonal rings are pictured). A natural local coordinate system for describing an Sb_4 unit is to let it lie in the $x-y$ plane; then the p_z orbitals we will discuss will be oriented perpendicular to the

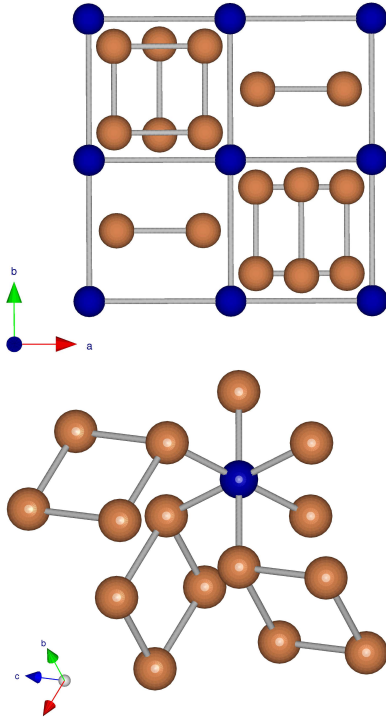


FIG. 2: (Color online) Top: view down a cubic axis of CoSb_3 , illustrating the very regular appearing positions of the Sb_4 rings, drawn as connected by bonds. Note that one of these rings looks like a dumbbell when viewed edge on. The (dark) Co atom is pictured without bonds. Bottom: an indication of the environment of the Co atom (smaller sphere); only three of the six attached Sb_4 rings are pictured. In this structure, all Sb sites are equivalent as are all Co sites.

plane of the Sb unit. The p_x, p_y orbitals are nearly symmetry related and naturally lead to bonding and antibonding molecular orbitals, and hence are very similar in character, while the nonbonding p_z orbitals have distinctive character.

If the origin is chosen so the large empty sites are centered at $(\frac{1}{4}, \frac{1}{4}, \frac{1}{4})$ and $(\frac{3}{4}, \frac{3}{4}, \frac{3}{4})$, then the rings are centered in each of the other subcubes $(\frac{1}{4}, \frac{3}{4}, \frac{3}{4})$ etc. A ring oriented perpendicular to \hat{z} is neighbored by rings above and below ($\pm\hat{z}$ directions) oriented perpendicular to (say) \hat{y} , by rings in the $\pm\hat{x}$ directions perpendicular to \hat{x} , and neighbored by the empty sites along the $\pm\hat{y}$ directions. A symmetric combination of the four p_z orbitals on a ring, call it P_z , is orthogonal to the P_z orbitals on neighboring rings, so if dispersion is governed by inter-ring hopping (rather than through Co atoms) some rather flat Sb p_z bands should result. Such behavior is seen in fatbands plots (see below).

As mentioned, the skutterudite structure is re-

lated to the perovskite structure $\square\text{TPn}_3$ (\square denotes an empty A site). Beginning from perovskite, a rotation of the octahedra keeping the Pn atoms along the cube faces results in the formation of the (nearly square) Pn_4 rings, and the Pn octahedra become distorted and less identifiable as a structural feature. The transformation is, in terms of the internal coordinates u and v ,

$$u'(s) = \frac{1}{4} + s(u - \frac{1}{4}); \quad v'(s) = \frac{1}{4} + s(v - \frac{1}{4}). \quad (1)$$

The transformation path, from perovskite for $s=0$ to the observed structure for $s=1$, is pictured in Fig. 1 of Ref. 24. Below we make use of this transformation to follow the opening of the (pseudo)gap between occupied and unoccupied states.

III. COMPUTATIONAL METHODS

Two all-electron full-potential codes, FPLO-9²⁵ and WIEN2k²⁶ based on the augmented plane wave+local orbitals (APW+lo) method,²⁷ have been used in these calculations, with consistent results. The Brillouin zone was sampled with regular $12 \times 12 \times 12$ k -mesh during self-consistency. For WIEN2k, the basis size was determined by $R_{mt}K_{max} = 7$. Atomic radii used were 2.50 a.u. for Co and 2.23 a.u. for Sb, and the Perdew-Wang form²⁸ of exchange-correlation functional was used. The experimental lattice parameters and atomic positions were taken from Ref. 20–22.

IV. PEROVSKITE TO SKUTTERUDITE TRANSFORMATION

The development of the electronic spectrum as the crystal is distorted from perovskite to the skutterudite structure is pictured in the three panels of Fig. 3. For the ideal perovskite the result is a highly metallic state, with no gap or pseudogap near the Fermi level. The important features only arise near the end of the distortion path. For $s=0.75$ (top panel of Fig. 3) the valence bands have just become disjoint from the conduction band and gap formation is imminent. For $s=0.90$ the gap is well formed and the minimum direct gap is emerging at the Γ point. The unusual high velocity band arising from the Γ point, already striking at $s=0.75$, remains unchanged at this point. The valence bands are a mass of indecipherable spaghetti.

By $s=0.95$ (bottom panel) a similarly high velocity band is emerging from the valence bands to the maximum at the Γ point. At $s=1.0$ it becomes

clear that it is a partner of the high velocity conduction band, as discussed in our earlier paper¹⁰ and to which we return in the next section. No doubt the formation of the gap, *i.e.* formation of occupied bonding bands and unoccupied antibonding bands, is behind the stability of the skutterudite structure in the Co pnictides class of materials. The fact that the gap only opens as the Sb p_x and p_y bonding-antibonding splitting becomes strong supports the picture that this $t_{pp\sigma}$ interaction takes precedence over the Co-Sb interactions within the CoSb_6 unit; however, these latter interactions (*i.e.* the presence of the Co atom) are necessary for the gap formation.

V. ELECTRONIC STRUCTURE

A. The Zintl Viewpoint

Although in the ‘parent’ perovskite system the structure is that of vertex-connected CoSb_6 octahedra, in the strongly distorted skutterudite structure the Sb_4 rings form a basic structural motif. These compounds, *viz.* CoSb_3 , are sometimes characterized as Zintl materials in which the Sb_4 unit balances the charge of the Co unit. Within the Zintl picture, the charge of the Co^{m+} ion must be balanced by a $(\text{Sb}_4)^{(4m/3)-}$ unit: there are only $3/4$ as many Sb_4 rings as Co atoms. Thus there is tension between the Zintl picture, which does not lead to integral formal charges on both of the primary units, and the presence of the gap that specifies an integral number of occupied bonding states. Several papers^{14,23,24,29–35} have presented results and some analysis for empty and for a few filled skutterudites. We have benefited from the previous work as we proceed on a deeper analysis.

We first follow the commonly held line of reasoning that the short Sb-Sb distance in the Sb_4 ring is the most fundamental aspect of the electronic structure.³⁵ The $p_x - p_x$ bonding along an x -axis is characterized by a hopping amplitude $t_{pp\sigma} \approx 3$ eV, so the corresponding bonding and antibonding states lie at $\varepsilon_p \pm t_{pp\sigma}$. The separation of Sb atoms and the σ bonding and antibonding between p_y orbitals along the y -direction is indistinguishable from that of the $p_x \sigma$ case. Indeed, the corresponding p_σ bonding and antibonding character (not shown in figures) is centered roughly ± 3 -4 eV below and above the gap. The on-site energies $\varepsilon_{p_x} \approx \varepsilon_{p_y} = \varepsilon_p$ therefore lie in the vicinity of the gap. This picture leads to half-filled p_x and p_y orbitals.

The p_z orbitals within an Sb_4 unit are orthogonal to the p_x, p_y orbitals and couple by a $t_{pp\pi}$ hopping

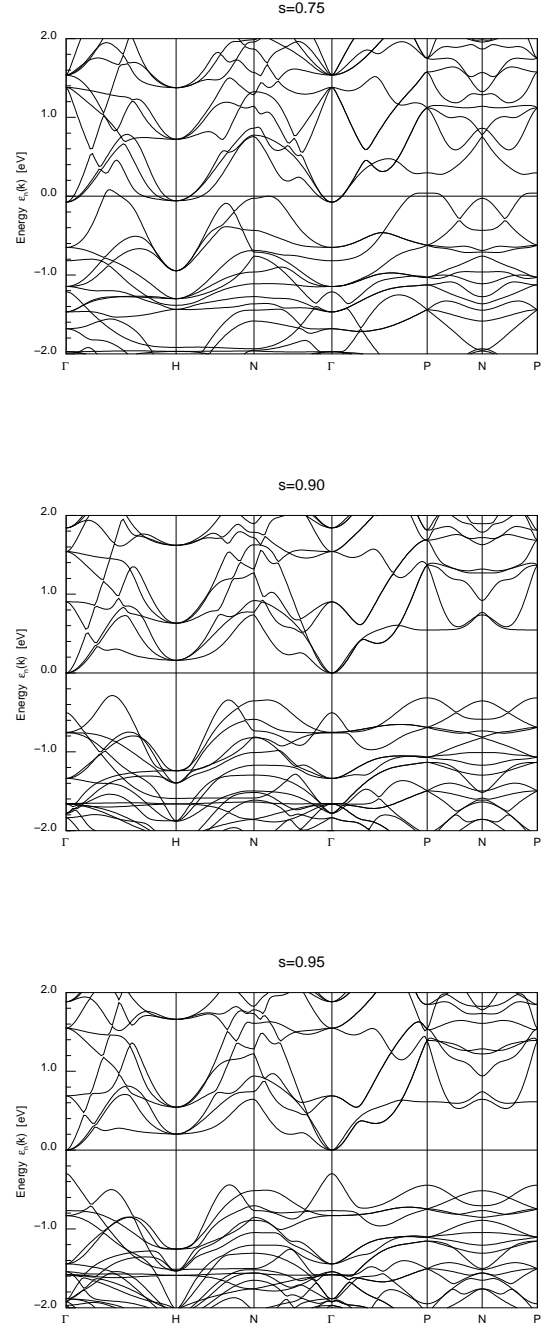


FIG. 3: Transformation of the band structure from metallic in the perovskite to semiconducting in the skutterudite, following the (linear) transformation described in the text. From the top, the panels show $s = 0.75, 0.90, 0.95$. The gap only begins to emerge around $s = 0.75$, where the conduction bands are already disjoint from the valence bands. The linear band near Γ emerges from the valence bands around $s = 0.95$.

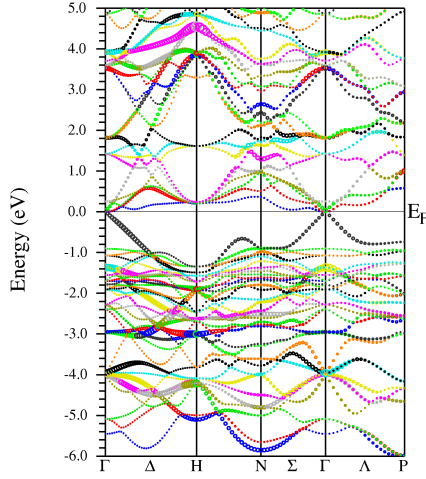


FIG. 4: (Color online) Band structure of CoSb₃ along high symmetry directions, with fatbands highlighting the Sb p_z character. The character is substantial in the -3 to -6 eV region, in the 3 to 5 eV region, but most notably in the linear band extending through the gap, which is primarily p_z in character.

amplitude. This coupling leads to doubly degenerate levels at $\pm t_{pp\pi}$ relative to ε_p . The evidence is that there is negligible crystal field splitting of the three on-site p orbitals. However, inter-unit $p_z - p_z$ interaction will be stronger than this intra-unit coupling, and the p_z orbitals also couple to the Co orbitals. The p_z character, provided by the fatbands representation in Fig. 4, is in fact distributed throughout the -6 eV to +5 eV region and is not reproducible by a simple model due to other couplings. The p_z projected density of states (DOS) indicates the p_z orbitals are at least half-filled, perhaps slightly more.

B. Complications with the Zintl Viewpoint

It is readily demonstrated that analysis focusing primarily on the Sb₄ rings has strong limitations. We have performed calculations with the Co atom removed, $\square\text{Sb}_3$. The Sb p band complex is broad (10 eV) and featureless. There is no hint of a gap or even pseudogap, indicating that the p_x and p_y bonding-antibonding feature described above is far from a dominant feature. Only when Co is re-inserted into the structure does the remarkably clean 1 eV gap become carved out around the Fermi level, except of course for the peculiar linear band near the zone center. The gap therefore arises from the Co $3d$ mixing (evidently strongly) with Sb $5p$ orbitals, with the linear band emerging from the valence bands being

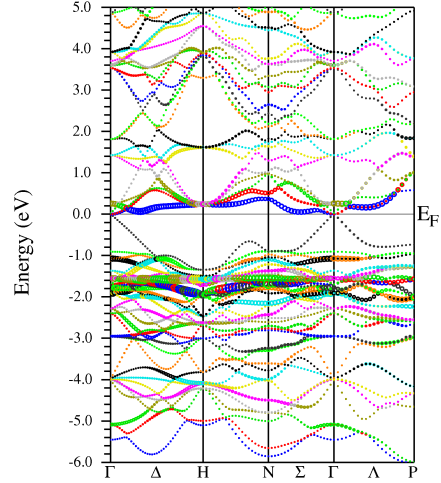


FIG. 5: (Color online) Band structure of CoSb₃ along high symmetry directions, with fatbands highlighting the Co $3d$ character. This plot reflects a narrow mass of d bands throughout the -1 to -2 eV range, more around -3 eV, and ~ 4 unoccupied bands in the 0-1 eV range. The amount of $3d$ occupation is discussed in the text.

of strong Sb character.

Figure 5 illustrates the Co $3d$ character. It lies mostly below the gap, in the very narrow -1 to -2 eV range. A much smaller amount of character, roughly something like four bands, lies immediately above the gap in the 0-1 eV range. These two parts of the $3d$ projected DOS are neatly and impressively split by the 1 eV gap. The “charge state” (or formal valence, or oxidation state) of the Co atom is a question that can be asked, since this is an insulating material. If there are four unoccupied d bands (though this cannot be claimed very conclusively due to the strong hybridization) then considering there are four Co atoms in the cell, the occupation would be d^8 Co¹⁺. A nonmagnetic ion with this filling is natural for the Co $\bar{3}$ site symmetry. As the CoSb₆ octahedron is distorted strongly in progressing from the cubic perovskite structure to the skutterudite one, the crystal field levels reduce as $t_{2g} \rightarrow t_1 + t_2$, the latter being the doublet, and $e_g \rightarrow e_1 + e_2$. One unoccupied orbital singlet (both spins) gives the d^8 occupation. The magnetic quantum number $m = 0$ orbital with respect to the local three-fold axis is the natural one for the $3d$ holes to occupy.

Charge balance will then leave the rings as $(\text{Sb}_4)^{-4/3}$, a very unsatisfactory result for accounting for the gap: each Sb₄ ring would not have an integer number of (fully) occupied bands (or molecular orbitals). Within the picture that the p_x and p_y orbitals are half-filled due to the large $t_{pp\sigma}$ bonding-antibonding splitting, this Co charge state would

suggest p_z orbitals to be 1/6 more than half-filled, a peculiar result and one that would only be compatible with a metallic, rather than semiconducting, state.

The integrated DOS for the Co 3d states in fact gives a clear d^8 occupation. However, with near-neutral atoms there might be significant Co 4s, 4p occupation, which could bring Co nearer to a neutral d^8s^1 configuration. Some Co sp character is in fact found in the upper valence bands, though it is possible that this represents tails of Sb p orbitals. The Co d occupation d^8 is clear, however.

C. Sb 6p - Co 3d Mixing

It was noted above that when Co is removed from the structure, there is no gap nor any indication of one, nor any candidate for a potential linear band. The most direct interaction of the Sb p_z orbitals on the ring is between the p_z orbital on the nearest Sb in the ring with the rotated $xz \pm yz$ orbitals on the eight Co neighbors. Sb₆ molecular orbitals (MOs) formed by linear combinations of p_z orbitals can be sorted according to whether they are even or odd parity with respect to the center of inversion at the Co site. The even parity MOs mix with the Co 3d orbitals, forming bonding and antibonding pairs tending to open a gap; the odd parity MOs do not mix with the 3d orbitals. As a result of this coupling, four of the five 3d orbitals are lowered and occupied, while one is raised and unoccupied, giving the 1 eV gap and the d^8 occupation.

D. Band Character near the Gap

The fatbands representation of Sb p_z character in Fig. 4 shows the substantial p_z character of the linear band in the upper valence bands near the zone center. This p_z character is in fact the dominant character, although various other small contributions from other valence orbitals are mixed in by the low Sb site symmetry. The character of the 3-fold degenerate conduction band minimum state is more complex. These bands have primarily Co “ t_{2g} ” character; the quotes arise from the fact that the degeneracies of the cubic t_{2g} and e_g subshells are broken by the distortion of the octahedra in the skutterudite structure. There is a strongly d_{z^2} flat band just above (+0.2 eV) the gap, and additional strong $d_{x^2-y^2}$ character in the 0.2-0.6 eV region.

The band figures we show below demonstrate that the linear band couples to only one of the triplet of conduction bands at and near Γ , *i.e.* couples to only

one linear combination of the triplet states. It does not couple to the Co 3d orbitals.

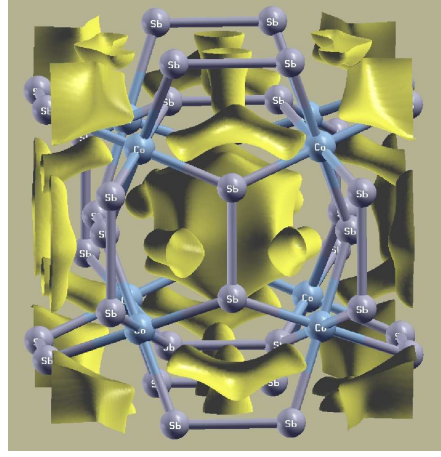


FIG. 6: Surface plot of the density arising from the linear band in CoSb₃ near $k=0$. The closed surface surrounds the unoccupied site in the skutterudite lattice and encloses a region of lower density than outside of the surface.

E. A consistent viewpoint: an empty-site molecular orbital

A generalized viewpoint of the most physical orbitals in CoSb₃ is that of four Co¹⁺ d^8 atoms (as discussed above), three Sb₄ rings with p_x - and p_y - σ bonding states filled and antibonding states unoccupied, and molecular orbitals formed from the twelve p_z orbitals and centered on the empty 2a site. This site is an inversion center, so the MOs can be classified as parity-even or -odd. (Note that these are different MOs than were discussed in Sec. V.C.) Twelve MOs can be formed, which can be classified also by the tetrahedral 2a site symmetry. Charge counting requires that eight of these MOs must be occupied (with both spins).

We will not attempt to identify the positions and dispersions of these MOs, except to note that linear band is one of these MOs. Jung *et al.*³⁵ identified this MO as A_{2u} , an orbitally nondegenerate state with odd parity at $k=0$, and therefore not mixing with the Co 3d orbitals at (or near) Γ . The density arising from this orbital is of interest. We had earlier investigated the possibility that an electron may reside in the large empty 2a site in the skutterudite structure. This type of “electride” configuration, in which an interstitial electron without a nucleus becomes an anion, is well established in molecular

solids.^{36,37} However, the density at the $2a$ site is very small, ruling out this possibility.

An isosurface plot of the density arising from the linear band near Γ is shown in Fig. 6. The closed surface in the density encloses a region of *low density* centered on the unoccupied site. Exploring the density with isosurfaces at various values of density reveals no local maximum at this large interstitial site, thus no electrone-like character. Lefebvre-Devos *et al.* have presented³⁰ complementary isosurface density plots of this band, with the high density regions of two types. One region surrounds the empty site (with rather complex shape) consistent with its origin as a MO comprised of p_z Sb_4 ring states, with the tetrahedral symmetry of the $2a$ site. The second region is within each CoSb_6 octahedron, centered on either side of the Co atom along the local $\bar{3}$ axis, appearing as a three-bladed propeller that arises from the lobes of the p_z orbitals that lie closer to the Co atom.

Interaction of the p_z states with Co $3d$ orbitals appears to cause a majority of the density of this state to border the large empty site. The result is not an electrone state but rather a large molecular orbital (one of twelve in total) centered on the empty site, with one of them (A_{2u}) per primitive cell. We have previously reported that this state at Γ is parity-odd.¹⁰

Such an orbital has the same hopping amplitude t along each nearest neighbor direction on a *bcc* lattice, hence its dispersion looks like that of an s orbital, $E_k = 8t \cos(k_x a/2) \cos(k_y a/2) \cos(k_z a/2)$, and does not lead to a linear band at $k=0$. This shouldn't be surprising, as the true linearity at Γ is accidental, due to a degeneracy that has to be tuned. In our previous paper,¹⁰ this tuning was accomplished by making two on-site energies in the tight-binding model identical.

The “linear band” aspect of the skutterudites may have been over-interpreted, because it arose in the most common member (the mineral skutterudite CoAs_3) which was studied most heavily initially. In a general skutterudite, for example the filled one $\text{LaFe}_4\text{P}_{12}$, the same band rises out of the valence band complex but is not unduly “linear.” The iso-valent members XPn_3 , with $X = \text{Co}, \text{Rh}, \text{Ir}$, and pnictides $\text{Pn} = \text{As}$ and Sb , all seem to lie not far from the critical degeneracy that extends the band linearly to $k=0$; however, we know of nothing in general about the skutterudite crystal structure that otherwise promotes a linear band.

VI. NONANALYTICITY, ANISOTROPY, AND THE TOPOLOGICAL INSULATOR PHASE

A. Band Inversion: Internal strain, spin-orbit coupling, and tetragonal strain

In previous work¹⁰ we demonstrated that it is possible, with very small Sb sublattice displacement (see Sec. II for the linear distortion, characterized by the parameter s), for this band to remain linear all the way to $k=0$, marking a critical point. In that work, the progression of the band crossing at the critical point was plotted. Due to the 3-fold degeneracy of the conducting band edge, the progression versus s was from semiconductor for $s \leq 1.19$, to the critical point at $s=1.020$ with linear *valence and conduction* bands degenerate with two quadratic bands, to a zero-gap semiconductor for $s \geq 1.021$ due to a symmetry-determined degeneracy, even when spin-orbit coupling (SOC) is included. Due to the band inversion and the character of the states at Γ , the transition is from trivial insulator to one with topological character. Because the degeneracy at the point Fermi surface (at Γ) remains, the latter state is a topological zero-gap semiconductor rather than a topological insulator.

We now demonstrate that a simple tetragonal distortion, such as might result from growth on a substrate with small lattice mismatch, does produce a topological insulator (TI) but with an unexpected placement of the gap. The progression of the band structure very near Γ is shown in Figure 7 for strain $c/a=1.01$. The gap before the critical point is reached always has quadratic bands for sufficiently small k . At the critical point $s = 1.020$ (when the strain is imposed) leads, unexpectedly, to linear bands only in certain of the high symmetry directions (such as the $\langle 111 \rangle$ direction, toward the P point). In other high symmetry directions (from Γ toward H is pictured) the bands are quadratic and the upper one is quite flat (heavy mass). We return to this point in the next subsection.

Beyond the critical point, the four bands become non-degenerate once more; the lower (linear) band has crossed the lowest of the three conduction bands and acquired mixed character. The coupling between bands is clearly much smaller along the axes (Γ -H direction) than along the other symmetry lines, and the gap occurs along this direction. Because of the heavy mass of the lower conduction bands, the gap is quite small, being of the order of 1 meV for the tetragonal strain that is pictured in Fig. 7.

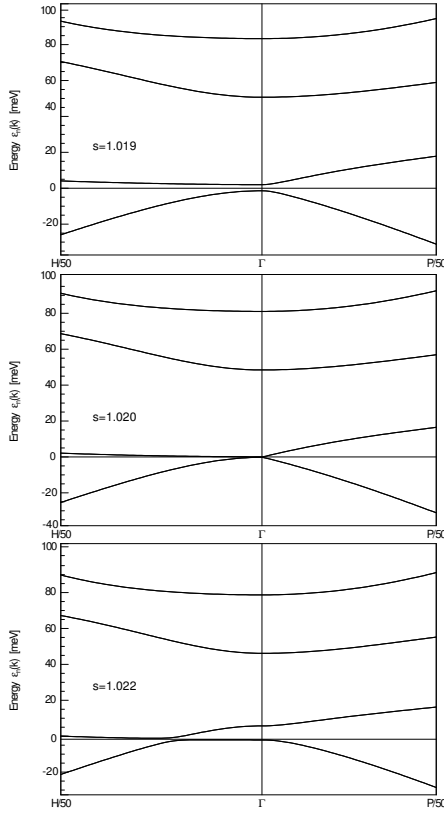


FIG. 7: Transformation of the band structure very near $k=0$ from insulating at $s=1.019$ (top) through the semimetallic critical point at $s=1.020$ to the inverted band insulator at $s=1.022$ (bottom). H/50 and P/50 denotes the point 2% of the way from Γ to H and P, respectively. The horizontal line lies in the gap (or at the Fermi level) in each panel. In the bottom panel the gap has moved out along the Γ -H line but is non-vanishing. The much larger band repulsion along Γ -P produces the unique band dispersion at the critical point.

B. Anisotropy at the Critical Point

Inspecting the bands along the three cubic high symmetry directions, a second peculiar feature becomes evident. At the critical point, the “linear band” disperses linearly along the $\langle 111 \rangle$ directions, while they are quadratic (with distinct masses) along both the $\langle 100 \rangle$ and $\langle 110 \rangle$ directions. The directional dependence as well as the magnitude dependence of the wavevector is anomalous. The form of the dispersion for small $|\vec{k}|$ can be constructed. A polynomial in the direction of \vec{k} (\hat{k}) with cubic symmetry that vanishes along the

$\langle 100 \rangle$ directions can be constructed as

$$P_{100}(\hat{k}) = \sqrt{\prod_{j=1}^6 (\hat{k} - \hat{k}_j)^2} = \prod_{j=1}^6 |\hat{k} - \hat{k}_j|, \quad (2)$$

where $\{\hat{k}_j\}$ are the six $\langle 100 \rangle$ unit vectors. The denominator normalizes the polynomial to unity along each of the $\langle 111 \rangle$ directions; \hat{k}_{111} lies along the $\langle 111 \rangle$ direction (any of them). The analogous polynomial $P_{110}(\hat{k})$ that vanishes along each $\langle 110 \rangle$ direction and is normalized to unity along each $\langle 111 \rangle$ direction can be constructed. Then the peculiar band pair is given by

$$\varepsilon(\vec{k}) = \pm v |\vec{k}| P_{100}(\hat{k}) P_{110}(\hat{k}) + \frac{k^2}{2m_s} \pm \frac{k^2}{2m_a}, \quad (3)$$

where m_s, m_a serve as symmetric and antisymmetric masses.

C. Isovalent Skutterudite Antimonides

We have studied the band structures of antimonide sisters of CoSb_3 , based on the transition metal atoms Rh and Ir. Band structures, or sometimes only gap values, of these compounds have been reported earlier.^{23,31,38} The band structures around the gap at $k=0$ differ somewhat in the literature, due to sensitivity to structure (and that some use relaxed coordinates while others use the measured structure), to the level of convergence of the calculation, and the exchange-correlation functional.

The difference in lattice constant is compensated very closely by the effect of difference in interatomic distances on hopping amplitudes, and the resulting bands are very similar. The single feature of interest is the magnitude of the gap (and whether positive or negative, the latter giving an inverted band structure) and the strength of SOC effects. As mentioned above, band inversion alone does not in itself give rise to a topological insulator state in these compounds because even after SOC is included, a two-fold degeneracy at Γ is lowest and the system is a point Fermi surface, zero-gap semiconductor. Such cases are referred to as topological semimetals. However as shown above, the topological semimetal can be driven into the TI phase by tetragonal distortion that lifts the final degeneracy.

RhSb₃. For a range of volumes around the experimental one ($a = 9.23 \text{ \AA}$), this compound has an inverted band structure, hence it is a point Fermi

surface, zero-gap topological semimetal. In the inverted band structure before considering SOC, the singlet lies 23 meV above the triplet that pins the Fermi level. Inclusion of SOC leaves the Fermi energy pinned to a doublet. A tetragonal distortion raises the degeneracy; a topological insulator is obtained for $c/a > 1$ in the same way that happens for CoSb₃ although no sublattice strain is required in RhSb₃.

Generally, reducing volume (applying pressure) in these Sb-based skutterudites leads to a larger gap. In the case of RhSb₃, our calculations indicate a gap never actually opens within cubic symmetry, for peripheral reasons. When the band inversion at Γ is undone and a gap at Γ appears at sufficiently high pressure ($a = 9.06 \text{ \AA}$), the material is metallic due to other (Rh $4d$) bands having become lowered in energy, crossing the Fermi level along the Γ -N direction.

IrSb₃. The larger SOC for heavier atoms led us to consider this $5d$ compound. However, the linear band and several others have practically no metal atom character and are not affected by its spin-orbit strength. We obtain, using the same computational methods as for the other two compounds, that like CoSb₃, IrSb₃ has a ~ 80 meV gap and therefore no topological character at the experimental equilibrium structure. Like CoSb₃, it can be driven to an inverted band structure and hence topological character by internal and tetragonal strains.

VII. SUMMARY

One goal of this work was to provide a simple but faithful picture of the electronic structure of CoSb₃: the origin of the gap and the character of the linear band being the most basic. The picture is this. Co is in a d^8 configuration, leaving four electrons in the

Co₄Sb₁₂ unit cell to go into other bands. The p_x and p_y orbitals on the Sb₄ ring form strongly bonding (occupied) and antibonding (unoccupied) states, accounting for two of the three $5p$ electrons of each Sb atom, for a total of twelve occupied σ -bonding states (of each spin). The twelve π -oriented p_z orbitals couple between units as well as with the Co $3d$ orbitals, and form “molecular orbitals” centered on the vacant $2a$ sites in the skutterudites lattice. Eight of these MOs are occupied by 16 electrons, one from each Sb and one from each Co. The linear band is best pictured as arising from the coupling and dispersion of these MOs.

We have also justified our earlier statement¹⁰ that CoSb₃ is very near a conventional-to-topological transition. A small symmetry-preserving internal strain, a small applied tetragonal strain, and spin-orbit coupling drives CoSb₃ into a topological insulator phase. This critical point also marks a point of accidental (but tunable, by the strains) degeneracy that gives rise to emergence of linear Dirac-Weyl bands emanating from $k=0$, where they are degenerate with massive bands. At this critical point, the dispersion is non-analytic at $k=0$ and anisotropy is extreme, with the mass varying from normal to vanishing. In this respect CoSb₃ at its critical point bears several similarities to the semi-Dirac (Dirac-Weyl) behavior encountered^{39–41} in ultrathin layers of VO₂.

VIII. ACKNOWLEDGMENTS

We acknowledge illuminating discussions with S. Banerjee, R. R. P. Singh, C. Felser, and L. Mchler. Work at UC Davis was supported by DOE Grant DE-FG02-04ER46111. V.P. acknowledges support from the Spanish Government through the Ramn y Cajal Program.

¹ I. M. Tsidilkovski, *Gapless Semiconductors: a New Class of Materials* (Akademie-Verlag, Berlin, 1988).

² A. K. Geim and K. S. Novoselov, *Nature Mater.* **6**, 183 (2007).

³ A. H. Castro Neto, F. Guinea, N. M. R. Peres, K. S. Novoselov, and A. K. Geim, *Rev. Mod. Phys.* **81**, 109 (2009).

⁴ L. Fu, C. L. Kane, and E. J. Mele, *Phys. Rev. Lett.* **98**, 106803 (2007).

⁵ M. Z. Hasan and C. L. Kane, *Rev. Mod. Phys.* **82**, 3045 (2010).

⁶ X.-L. Qi and S.-C. Zhang, *Rev. Mod. Phys.* **83**, 1057 (2011).

⁷ D. Xiao, M.-C. Chang, and Q. Niu, *Rev. Mod. Phys.* **82**, 1959 (2010).

⁸ J. E. Moore, *Nature* **464**, 194 (2010).

⁹ X.-L. Qi, T. L. Hughes, and S.-C. Zhang, *Phys. Rev. B* **78**, 195424 (2008).

¹⁰ J. C. Smith, S. Banerjee, V. Pardo, and W. E. Pickett, *Phys. Rev. Lett.* **106**, 056401 (2011).

¹¹ P. Larson, V. A. Greanya, W. C. Tonjes, R. Liu, S. D. Mahanti, and C. G. Olson, *Phys. Rev. B* **65**, 085108 (2002); C.-X. Liu, X.-L. Qi, H. J. Zhang, X. Dai, Z. Fang, and S.-C. Zhang, *Phys. Rev. B* **82**, 045122 (2010).

¹² C. Liu, T. L. Hughes, X.-L. Qi, K. Wang, and S.-C. Zhang, *Phys. Rev. Lett.* **100**, 236601 (2008).

¹³ G. Xu, H. Weng, Z. Wang, X. Dai, and Z. Fang, *Phys. Rev. Lett.* **107**, 186806 (2011).

¹⁴ D. J. Singh and W. E. Pickett, *Phys. Rev. B* **50**,

- 11235(R) (1994).
- ¹⁵ T. Caillat, A. Borshchevsky, and J.-P. Fleurial, *J. Appl. Phys.* **80**, 4442 (1996).
 - ¹⁶ G. S. Nolas, D. T. Morelli, and T. M. Tritt, *Annu. Rev. Mater. Sci.* **29**, 89 (1999).
 - ¹⁷ B. C. Sales, D. Mandrus, and R. K. Williams, *Science* **272**, 1325 (1996).
 - ¹⁸ B. Yan, L. Muehler, X.-L. Qi, S.-C. Zhang, and C. Felser, *Phys. Rev. B* (in press); arXiv:1104.0641.
 - ¹⁹ P.-C. Ho, N. A. Frederick, V. S. Zapf, E. D. Bauer, T. D. Do, M. B. Maple, A. D. Christianson and A. H. Lacerda, *Phys. Rev. B* **67**, 180508(R) (2003).
 - ²⁰ K. Koga, K. Akai, K. Oshiro, and M. Matsuura, *Phys. Rev. B* **71**, 155119 (2005).
 - ²¹ T. Schmidt, G. Gliche, and H. D. Lutz, *Acta Crystallogr., Sect. C: Cryst. Struct. Commun.* **43**, 1678 (1987).
 - ²² A. Kjekshus and T. Rakke, *Acta Chemica Scand.* **28A**, 99 (1978).
 - ²³ H. Harima and K. Takegahara, *J. Phys.: Condens. Matter* **15**, S2081 (2003).
 - ²⁴ M. Llunell, P. Alemany, S. Alvarez, V. P. Zhukov, and A. Vernes, *Phys. Rev. B* **53**, 10605 (1996).
 - ²⁵ K. Koepf and H. Eschrig, *Phys. Rev. B* **59**, 1743 (1999).
 - ²⁶ K. Schwarz and P. Blaha, *Comp. Mat. Sci.* **28**, 259 (2003).
 - ²⁷ E. Sjöstedt, L. Nördstrom, and D. J. Singh, *Solid State Commun.* **114**, 15 (2000).
 - ²⁸ J. P. Perdew and Y. Wang, *Phys. Rev. B* **45**, 13244 (1992).
 - ²⁹ J. O. Sofo and G. D. Mahan, *Phys. Rev. B* **58**, 15620 (1998).
 - ³⁰ I. Lefebvre-Devos, M. Lassalle, X. Wallart, J. Olivier-Fourcade, L. Monconduit, and J. C. Jumas, *Phys. Rev. B* **63**, 125110 (2001).
 - ³¹ K. Koga, K. Akai, K. Oshiro, and M. Matsuura, *Phys. Rev. B* **71**, 155119 (2005).
 - ³² W. Wei, Z. Y. Wang, L. L. Wang, H. J. Liu, R. Xiong, J. Shi, H. Li, and X. F. Tang, *J. Phys. D: Appl. Phys.* **42**, 115403 (2009).
 - ³³ P.-X. Lu, Q.-H. Ma, Y. Li, and X. Hu, *J. Magn. Magn. Mat.* **322**, 3080 (2010).
 - ³⁴ D. Wee, B. Kozinsky, N. Marzari, and M. Fornari, *Phys. Rev. B* **81**, 045204 (2010).
 - ³⁵ D. Jung, M.-H. Whangbo, and S. Alvarez, *Inorg. Chem.* **29**, 2252 (1990).
 - ³⁶ D. J. Singh, H. Krakauer, C. Haas, and W. E. Pickett, *Nature* **365**, 39 (1993).
 - ³⁷ J. L. Dye, *Science* **247**, 663 (1990).
 - ³⁸ K. Takegahara and H. Harima, *Physica B* **328**, 74 (2003).
 - ³⁹ V. Pardo and W. E. Pickett, *Phys. Rev. Lett.* **102**, 166803 (2009).
 - ⁴⁰ S. Banerjee, R. R. P. Singh, V. Pardo, and W. E. Pickett, *Phys. Rev. Lett.* **103**, 016402 (2009).
 - ⁴¹ V. Pardo and W. E. Pickett, *Phys. Rev. B* **81**, 035111 (2010).